DOI 10.31489/2023PH3/75-85

UDC 55.23.13

Z. Berkinova, B. Golman*

School of Engineering and Digital Sciences, Nazarbayev University, Kabanbay Batyr ave. 53, Astana, 010000, Kazakhstan
*(*E-mail: boris.golman@nu.edu.kz)*

Flow Behavior of Complex-Shaped Particle Mixtures in Rotary Drums: A DEM Study

Metal matrix composites hold great potential as functional materials for energy conservation applications. These composites are manufactured using powder metallurgy, which involves the incorporation of fine particles with diverse shapes. Understanding the flowability of particle mixtures with varying shapes is crucial for optimizing industrial processes. This study focuses on analyzing the flowability and flow behavior of mixtures composed of alumina and aluminum alloy particles using the discrete element method. The particle shapes are modeled to closely resemble actual particles, and their flow behavior in a rotating drum is simulated. The upper and lower dynamic angles of repose, outlines of particle bed surface, particle displacements, and particle velocity distributions were analyzed to understand the flow characteristics of complex-shaped particles. The results reveal the influence of particle shape on the flow behavior of powder mixtures, providing valuable insights for process optimization and design.

Keywords: Complex shaped particles, powder mixtures, metal matrix composites, rotary drum, discrete element method, flowability, dynamic angle of repose, flow behavior.

Introduction

Granular materials have a wide range of applications in various industrial processes, such as additive manufacturing, powder metallurgy, pharmaceuticals, agriculture, and food engineering. Advanced functional materials, such as metal matrix composites, are commonly manufactured using powder metallurgy techniques [1]. Ceramic-reinforced metal matrix composites, in particular, hold great promise for energy applications owing to their lightweight nature and high strength [2]. The raw powder comes in different shapes, from simple spherical particles to complex elongated, bulky, and flaky particles. The shape of particles significantly affects various aspects of powder behavior, including powder flow dynamics [3], mixing rate [4], flow patterns [5], and particle breakage [6].

Flowability is a crucial property of bulk materials that can greatly impact both the production process and the functionality of various products. Powder flowability depends on several factors, such as particle shape and size distribution, the composition of the powder mixture, and environmental conditions. Various experimental techniques exist for measuring powder flowability, and their choice depends on the specific application. One effective method involves using a drum filled with powder that continuously rotates at low speeds, such as 4 rpm [7], 0-65 rpm [8], 5-20 rpm [9], and 6, 9, and 12 rpm [10], to measure the dynamic angle of repose of the powder.

The Discrete Element Method (DEM) has recently gained extensive use in studying the flow behavior of granular materials. However, many researchers rely on simplified models of particle shapes, such as spherical or ellipsoidal particles [11]. Unfortunately, these models may not accurately represent the shape of actual particles. Simulating the motion of irregular-shaped particles is computationally expensive and requires significant computational resources. Despite these challenges, a few studies have focused on complex-shaped particles. For example, Norouzi et al. [10] conducted research on the flow behavior of oval, oblong, and biconvex-shaped particles using a rotary drum. Their investigation revealed that the transition from a rolling to a cascading flow regime depends not only on the size and filling level of the particles but also on their shape.

Despite the significance of understanding the flow behavior of particle mixtures in rotary drums, there remains a gap in research concerning the analysis of mixtures consisting of particles of varying shapes. Therefore, the present study aims to analyze the flowability and flow behavior of mixtures of two materials with varying particle shapes using DEM. The shape of particles is modeled to closely resemble the actual particles.We investigated the flowability of alumina and aluminum alloy particle mixtures. The upper and lower dynamic angles of repose were measured using a rotary drum. Furthermore, we analyzed the impact of

the composition of complex-shaped particle mixtures on the particle bed surface, particle displacements, and particle velocities.

Materials and Methods

Materials

The AlSi10Mg alloy powder was procured from Avimetal, China, while the aluminum oxide was obtained from Sigma-Aldrich, Switzerland. For this study, we utilized mixtures of alumina and alloy powders containing alumina weight percentages of 2 %, 6 % and 10 %.

Particle size distribution

The size distributions of alumina and aluminum alloy powders were measured using the laser diffraction particle analyzer, Mastersizer 3000 by Malvern Panalytical. The analyzer was used in combination with the Aero S dry disperser. The disperser was operated under a pressure of 0.5 bar and 1 bar for alumina and aluminum alloy, respectively. The volume-based size distributions of alumina and aluminum alloy powders are illustrated in Figure 1. The characteristic diameters and span of size distributions are listed in Table 1. The diameters d10, d50, and d90 represent the particle sizes at which 10 %, 50 %, and 90 % of the cumulative undersize distribution are achieved. The span value is calculated as follows:

$$Span = \frac{d_{90}-d_{10}}{d_{50}}. \quad (1)$$

The alumina powder has a significantly larger size than the aluminum alloy powder, although its size distribution is slightly narrower.

Table 1

Characteristic diameters and span of particle size distributions

Property	Al_2O_3	AlSi10Mg
d_{10}(μm)	64.4	27
d_{50}(μm)	99.1	44
d_{90}(μm)	149	70.1
Span	0.854	0.980

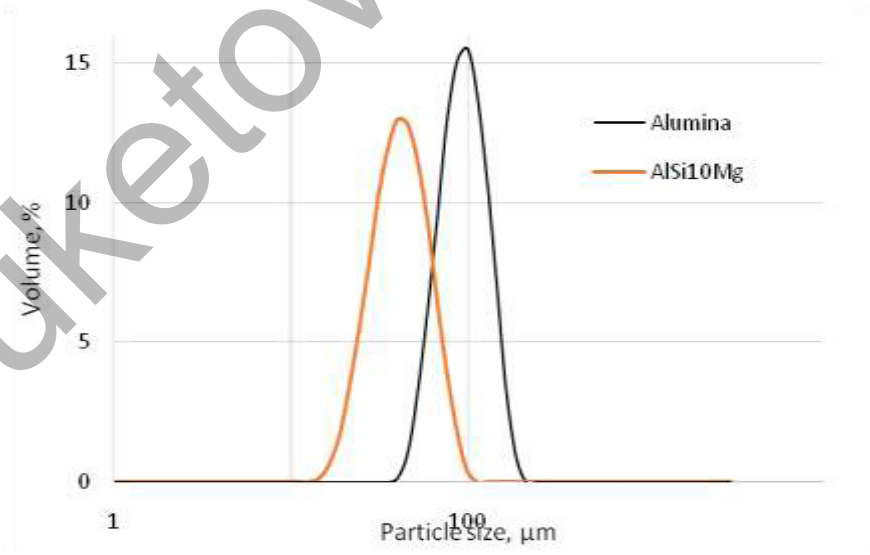

Figure 1. Size distribution of aluminum alloy and alumina particles

Particle morphology

The morphology of aluminum alloy and alumina particles was observed using a scanning electron microscope (SEM) provided by Zeiss Crossbeam 540, Switzerland. First, the samples were coated with carbon to protect the surface. Afterward, aluminum alloy particles were sputter coated with gold in a

Quorum Q150T ES to decrease charging during imaging. The SEM images of particles are illustrated in Figure 2.

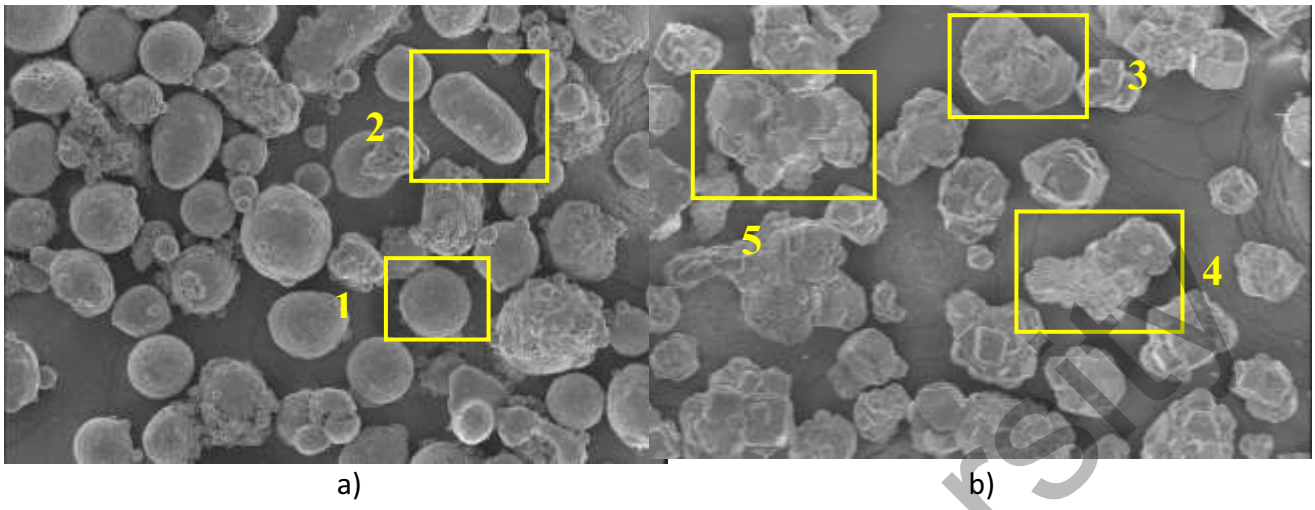

Figure 2. SEM images indicting outlined particle types of a) aluminum alloy and b) alumina particles

DEM contact model

The particle flow within the rotating drum was simulated numerically using DEM, initially proposed by Cundall and Strack [12]. DEM tracks the displacement and rotation of individual particles based on Newton's second law. Particle movement is described through translational and rotational motions as follows:

$$m_i \frac{dv_i}{dt} = \sum F_{c,i} + m_i g, \tag{2}$$

$$\frac{d(I_i \omega_i)}{dt} = R_i \left(\sum M_{c,i}\right). \tag{3}$$

Here, $m_i$denotes the mass of the particle, $F_{c,\,i}$ stands for the contact force v_i specifies the translational velocities, g is the acceleration of gravity, I_i is the moment of inertia, ω_i is the angular velocity vector, R_i is the torque acting on the body, and $M_{c,i}$ is the contact torque associated with rolling friction. The Hertz-Mindlin contact model, along with the elastic-plastic spring dashpot (EPSD2) rolling friction model, was employed to simulate particle-particle and particle-wall contacts. The elastic-plastic spring-dashpot (EPSD) rolling friction model has been formulated to consider additional torque contribution to the motion of particles. In this study, we used the EPSD2 model [13], which excludes the viscous damping torque component and considers only the mechanical spring torque, in contrast to the original EPSD model [14].

Particle model

A number of methods have been described in the literature for generating non-spherical particles for DEM simulation. Among these, the multi-sphere method [15, 16], which involves creating non-spherical particles by using clamps made of overlapping spheres with fixed local positions, and the superquadrics method [17-19], which generates particles of varying shapes by adjusting the parameters of superquadrics, are the most frequently employed. In the current study, the multi-sphere approach was utilized to generate particles of complex shapes. To enhance the accuracy of the obtained results, particle shapes for numerical simulation were generated based on SEM images and size distribution analysis of aluminum alloy and alumina particles.The aim was to simulate the shapes and sizes of particles as closely as possible to the actual particles. Two types of particle shapes were used for the aluminum alloy (Fig. 2a): spherical particles with a radius of 0.5 mm and elongated particles represented by five overlapping spheres, each with a constant radius of 0.4 mm (Fig. 3). Furthermore, to account for the bulky shapes and sharp edges of alumina particles, three types of complex-shaped particles were selected from the SEM image, as depicted in Figure 2b. Then, multi-sphere particles with shapes resembling the selected actual particles were generated using six, eight, and fifteen overlapping spheres, as illustrated in Figure 4.

(a) (b)

Figure 3. 3D model of generated aluminum alloy particles: a) sphere, b) elongated particle made of five overlapping spheres.

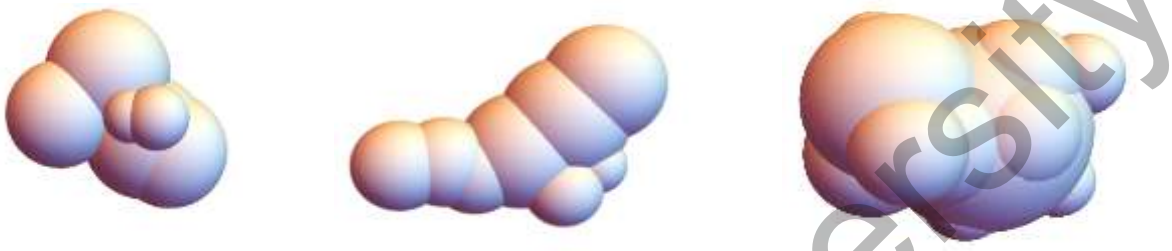

a) b) c)

Figure 4. 3D model of generated alumina particles consisiting: a) six overalapping spheres, b) eight overalapping spheres, c) fifteen overalapping spheres.

Particle insertion

The Aspherix software (DCS-Computing, Austria) was used to simulate the five cases. The first case involved aluminum alloy particles, the second case included alumina particles, and the other three cases represented mixtures of alumina and aluminum alloy particles, with 2 %, 6 %, and 10 % weight percentages of alumina powder.

The SEM images show that the aluminum alloy powder is composed mostly of spherical and elongated particles. For the DEM simulation runs 200,000 AlSi10Mg particles were randomly inserted into the simulation domain under normal gravity. Of all the particles, 60 % were spherical, while the remaining 40 % were elongated. In the case of pure alumina, 10,000 particles were inserted, with 50 % of them being multi-spherical particles consisting of eight overlapping spheres. The remaining two types of particles, with six and fifteen spheres, were evenly divided by 25 %.

To estimate the filling level of the drum, the volume of each particle in Table 2 was initially simulated by an analytical method using the Avro code developed by Busa et al. [20]. The results of these simulations are summarized in Table 2. Subsequently, the filling level of the drum was computed for each simulation case by utilizing the particle volume, the known number of particles of each type, and the volume of the drum used in the DEM simulations, as presented in Table 3. The filling level affects the flow behavior of particles in the drum and particle bed surface [8].

Table 2

Parameters of multi-sphere model for particle generation

Particle type	Number of overlapping spheres	Volume (mm^3)	Mass (g)
AlSi10M particles			
1	1	0.523	0.00116
2	5	0.66	0.00147
Alumina particles			
3	6	7.49	0.0280
4	8	13.12	0.0498
5	15	32.94	0.125

Table 3

Drum filling level of five simulation cases

Composite	Filling level (%)
Al_2O_3	38.8
AlSi10Mg	29.5
2 % Al_2O_3	28.3
6 % Al_2O_3	27.9
10 % Al_2O_3	27.4

Table 4 lists the material properties of the aluminum alloy and alumina particles, as well as the rotary drum. Stainless steel was chosen as the wall material for the drum to prevent electrostatic effects on the particles. The properties used in DEM simulations were selected to closely reflect real material properties, with one exception. Young's modulus (G) for the aluminum alloy was decreased from 7×10^7 Pa to 7×10^6 Pa to reduce computational time. This adjustment does not affect the results obtained, as noted by Chen [9].

Table 4

Material properties for particles and wall

Material property	$AlSi_{10}Mg$	Alumina	Rotary drum
Density, ρ (kg/m^3)	2230	3800	7500
Young's modulus, G (Pa)	7×10^6	3.2×10^7	1.8×10^7
Poisson's ration, v	0.3	0.23	0.3
Coefficient of restitution, e	0.75	0.4	0.7
Coefficient of friction, μ	0.3	0.6	0.3
Coefficient of rolling friction, μ_r	0.001	0.005	0.005

The rotary drum has a diameter of 200 mm and a thickness of 25 mm. To conduct the DEM simulations, particles were initially randomly distributed inside the drum and allowed to settle for 1 second to attain a stable position. Subsequently, the drum was rotated about *y*-axis at a constant speed of 20 rpm for 3 seconds. Finally, the dynamic angle of repose, which is the angle formed between the surface of a particle bed and the horizontal plane, was measured using the open-source software ImageJ.

To measure the upper and lower angles of repose in this study, the method proposed by Marigo and Stitt [21] and previously used by Jadidi et al. [22] was employed. The upper angle (α) was determined by drawing a line from the leftmost side to the center of the powder bed in the rotary drum, while the lower angle (β) was measured from the drum's center to the rightmost side. Figure 5 (a) shows a schematic representation of the drum in a stable position, while Figure 5 (b) depicts the drum during rotation about *y*-axis.

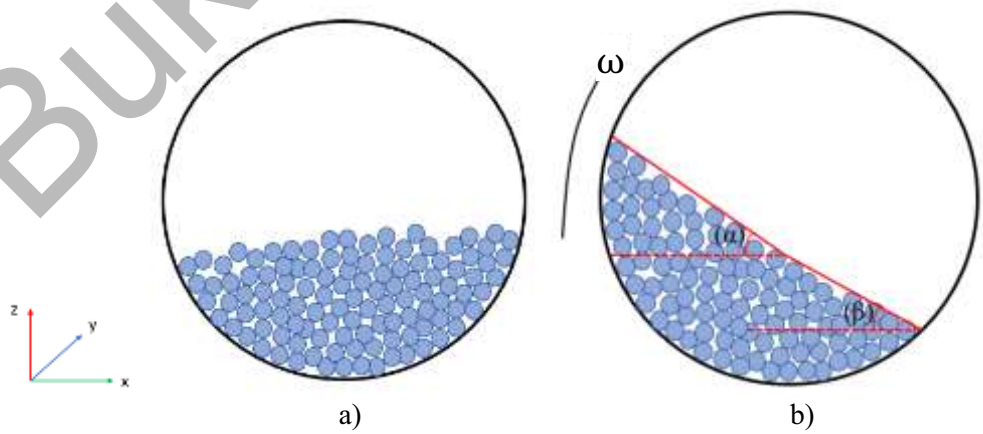

Figure 5. Schematic representation of a) drum in stable position b) drum during rotation about y-axis

Results and Discussion

Although the concept of a rotary drum is simple, the particle flow inside the drum is highly complex. Several studies [23, 24] have identified four distinct particle flow regimes: slipping, rolling, cascading, and cataracting. These regimes depend on various factors such as drum size, rotational speed, filling level, particle size distribution, and particle shape. To differentiate between these flow regimes in the rotary drum, the Froude number (*Fr*) is often used. The Froude number, given by $Fr = \omega^2 \cdot R/g$, characterizes the balance between gravitational and centrifugal forces. Here, ω represents the angular velocity in radians per second, and R denotes the radius of the rotating drum in meters. In our case, the *Fr* value is equal to 1.1×10^{-3}. The Froude number, along with the high filling level exceeding 10 % (as indicated in Table 3), suggests that the particle flow in the drumis in the cascading regime. This type of motion generates an S-curve particle bed surface, which is further supported by the DEM simulation results illustrated in Figure 6.

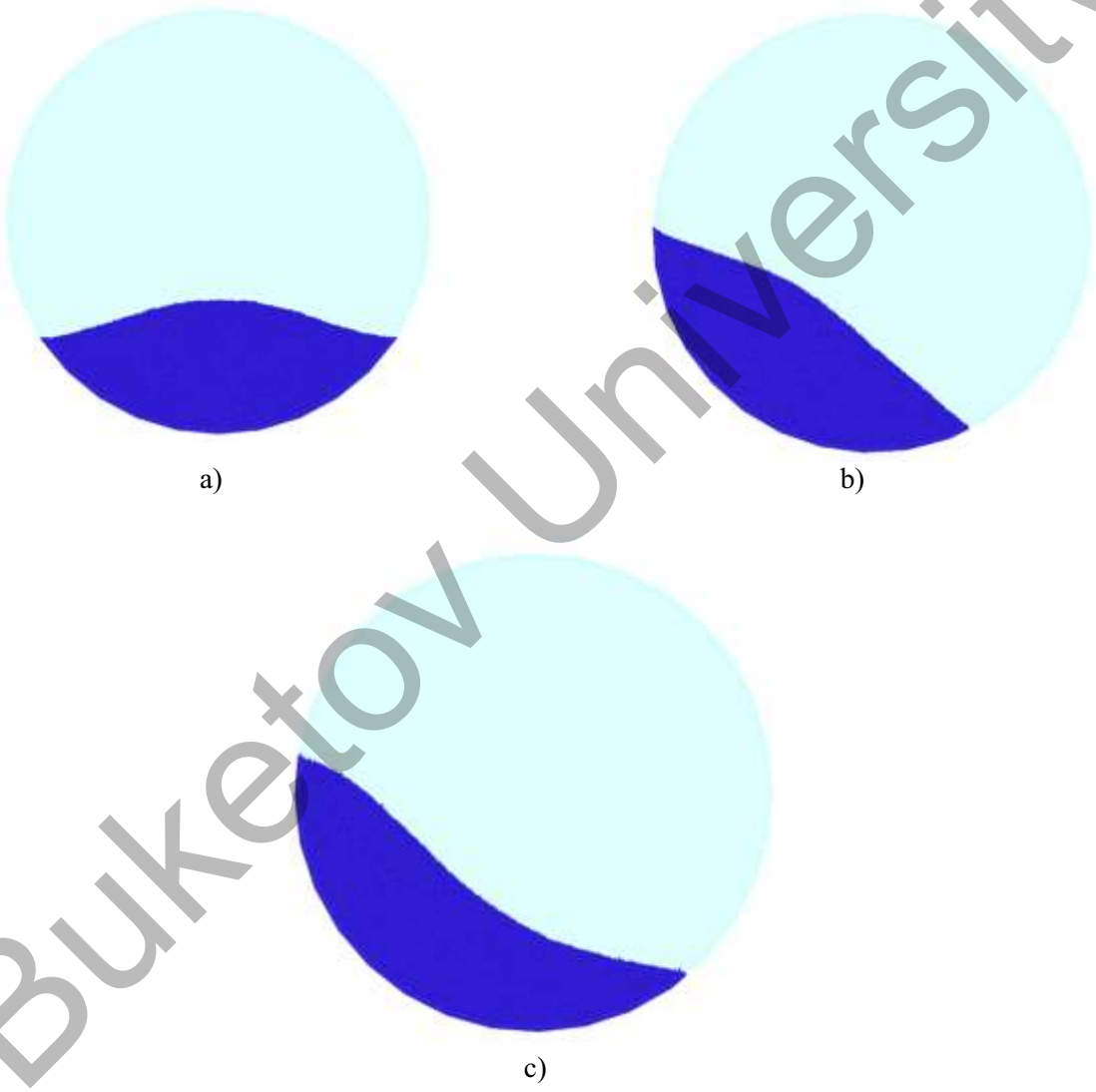

a) b) c)

Figure 6. Progressive visualization of cascading particle motion dynamics in rotating drum: a) particle insertion b) intermediate phase c) established cascading regime

Figure 7 illustrates the outlines of the particle bed surfaces formed in the rotating drum at various times. The bed surface outline was reconstructed from the DEM output files by detecting the maximum height of the particle bed in each bin along the *x*-axis direction. The higher and steeper surface outlines are detected for powder beds containing alumina particles (case 1). This can be attributed to the hardness and abrasiveness of alumina particles, which can increase inter-particle friction [25] and affect the behavior of the particle bed surface in the rotary drum. Moreover, the irregular shapes of alumina particles increase their

tendency to form clusters and aggregates within the powder bed, resulting in an uneven surface with steeper upper and lower angles of repose. This can be observed in the S-curve profile of the bed surface. On the other hand, aluminum alloy particles (case 2) have smoother surfaces, which can reduce the tendency for clustering and aggregation, resulting in a more uniform bed surface with less steep angles. This smoother bed surface may be observed as a more gradual change in slope and a more linear profile in comparison to the S-curve profile observed for alumina particles. The outlines of the bed surface for the mixtures of aluminum alloy and alumina particles (cases 3, 4, and 5) follow the trend of the aluminum alloy, displaying smooth bed surfaces. This can be attributed to the small amount of alumina added to the alloy, which is less than 10 %, as well as to the different filling levels of the drum.

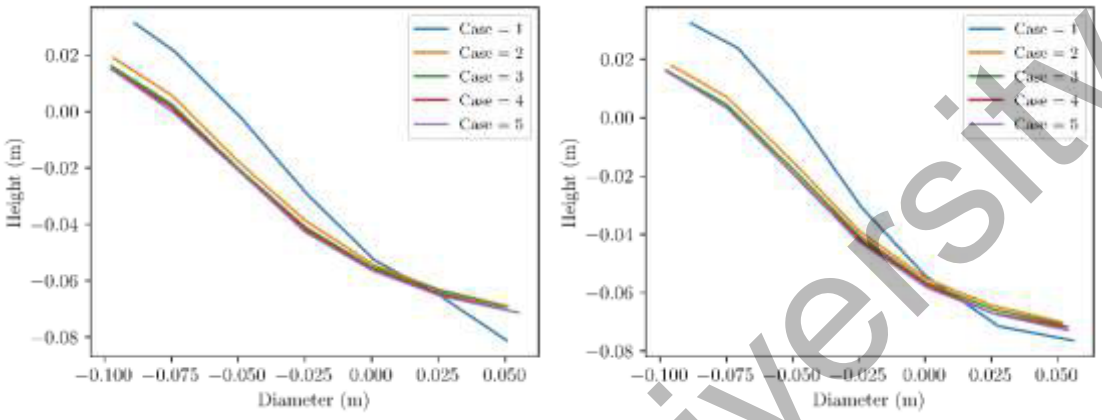

Figure 7. Particle bed surface profiles of AlSi10Mg, alumina, and their mixtures in drums after rotation for a) 1s and b) 3s

Table 5 summarizes the upper and lower dynamic angles of repose for aluminum alloy, alumina, and their mixtures, which were measured using ImageJ image analysis software on snapshots of DEM simulation results. The upper angles of repose exhibited a tendency to increase with simulation time in all cases. However, the lower angles of alumina particles decreased over time. The rotation of the drum's wall lifts the particles upward, but due to the high flow resistance, the particles encounter difficulties in freely flowing down. Consequently, the particles tend to accumulate and form a steeper pile in the upper region of the drum, while the lower region displays a flatter distribution of particles. Regarding the mixture of 10 % alumina particles in AlSi10Mg (case 5), we observed an initial increase in the lower angle of repose, which can be attributed to the addition of alumina particles. However, as time progressed, the lower angle of repose decreased, reaching a value lower than it was at 1 second. On the other hand, the upper and lower angles of repose for the other two powder mixtures (cases 3 and 4) increased with time, following the trend observed for the aluminum alloy particles. However, it should be noted that the angles of repose of the powder mixtures in both the upper and lower regions were smaller than those of the aluminum alloy particles. Despite the presence of alumina particles in the mixtures, the particle bed surfaces appeared flatter. This phenomenon can be attributed to the filling level of particles in the drum. A slight decrease in the filling level (refer to Table 3) could impact the flow of mixtures, resulting in increased angles of repose in the upper regions.

Table 5

Upper (α) and lower (β) dynamic angles of repose of aluminum alloy, alumina and their mixtures

Time, s	AlSi10Mg		Alumina		2 %		6 %		10 %	
	Dynamic angle of repose:									
	α	β	α	β	α	β	α	β	α	β
1	40.07	13.53	45.34	33.3	37.11	14.49	37.8	15.35	33.59	17.61
2	41.53	14.4	47.04	30.18	39.2	17.07	38.9	16.25	35.5	17.96
3	41.73	14.46	48.68	29.37	40.08	17.79	39.85	16.92	35.65	16.83

Additionally, the movement of particles during drum rotation was analyzed for each case. The maps of particle displacement magnitudes are shown in Figure 8 for cases 1 and 2. The magnitude of particle displacement is calculated using the Euclidian formula as follows:

$$d = \sqrt{(x_2 - x_1)^2 + (y_2 - y_1)^2 + (z_2 - z_1)^2}, \qquad (5)$$

where (x_1, y_1, z_1) and (x_2, y_2, z_2) denotes the particle positions at time t and $t + \Delta t$, respectively. The analysis of the displacement of alumina and aluminum alloy particles in the rotary drum suggests that there is a variation in mobility among particles located in different regions. Specifically, the results indicate that alumina particles in the drum's upper side exhibit greater mobility than those in the lower side. Moreover, the displacement of aluminum alloy particles is greater for particles positioned on the lower side of the drum compared to the alumina particles located in the same positions.

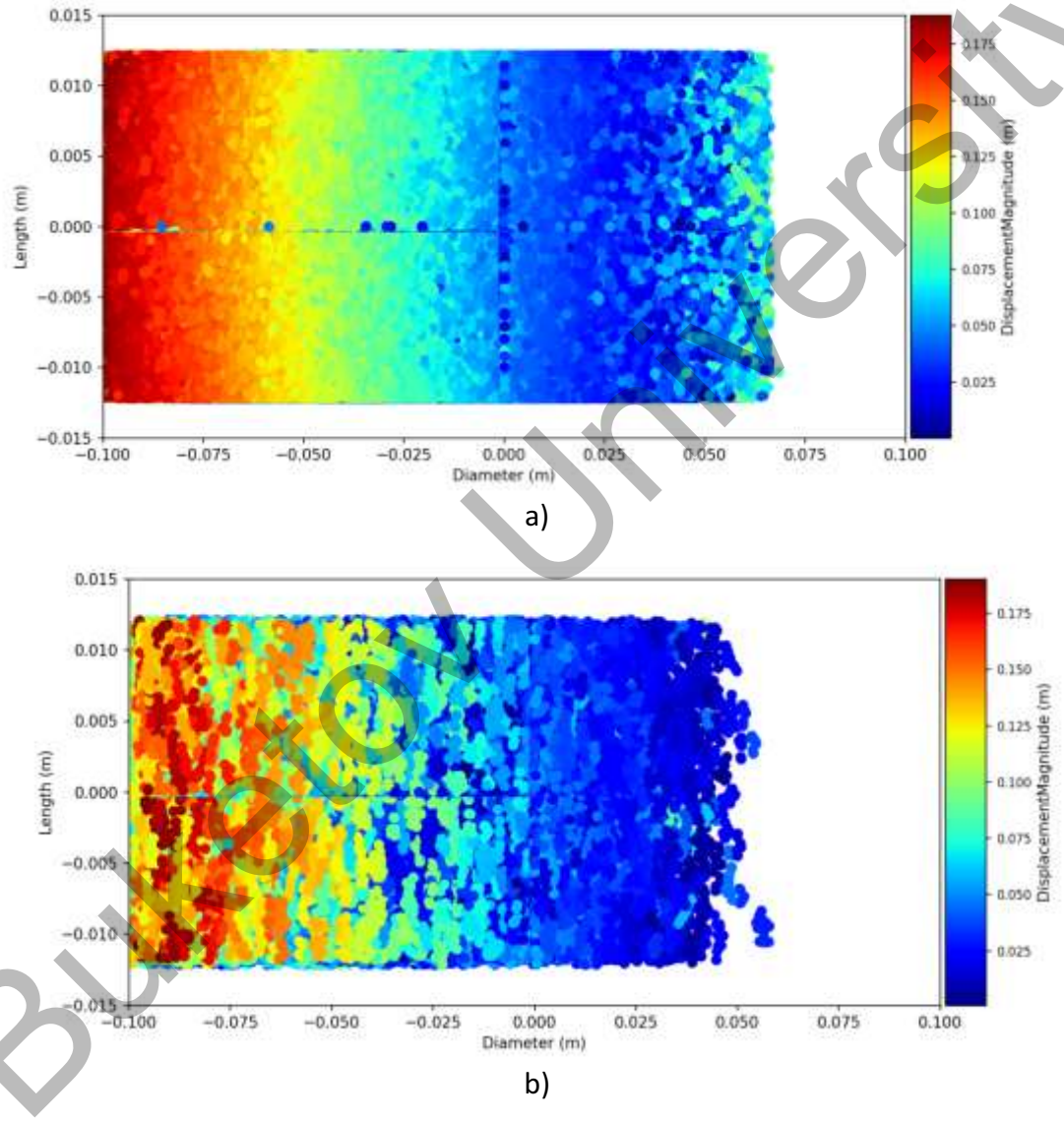

Figure 8. Maps of particle displacement magnitudes along the diameter and length of rotary drum for a) aluminum alloy and b) alumina particles

The particle velocity is an important parameter for predicting the flow behavior of particles. Figure 9 shows the maps of particle velocity magnitudes for aluminum alloy and alumina powders. Based on these magnitudes, the particle bed in the rotary drum can be divided into two layers: active and passive. The boundary between these layers is indicated by dark blue color, representing particles with velocities close to zero. Particles within the active layer flow downward due to gravitational force, while particles in the passive layer possess a tangent velocity equal to the velocity of the drum wall. This is a result of the no-slip condition at the drum wall. As particles move from the drum wall towards the center of the drum, their

velocities gradually increase and then subsequently decrease until they eventually match the velocity of the drum wall in the lower region. The velocity maps of mixtures containing alumina and aluminum alloy particles emphasize the dominant influence of the aluminum alloy particles. The mixtures tend to display velocity patterns that closely resemble those observed for pure aluminum alloy particles.

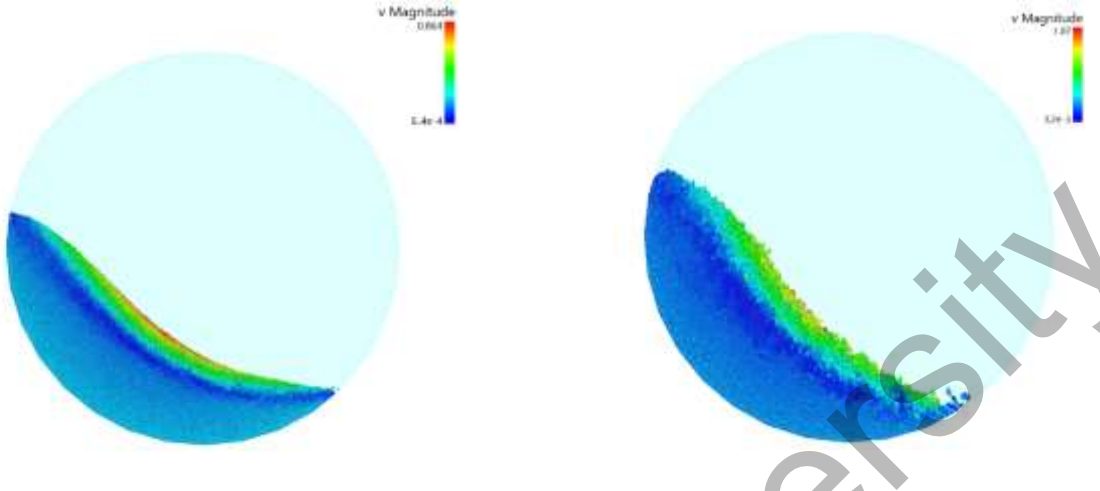

a) b)

Figure 9. Maps of velocity magnitudes of a) aluminum alloyand b) alumina particles in rotary drum

Conclusion

In this study, the flow behavior of mixtures of particles with different shapes in a rotating drum was analyzed employing DEM. The simulations were conducted for mixtures containing 2 %, 6 %, and 10 % alumina particles in aluminum alloy particles, as well as for pure alumina and pure aluminum alloy particles. To accurately represent the particle shapes, they were digitally replicated based on SEM images of actual particles, utilizing the multi-sphere method. Using the DEM simulation results, the upper and lower dynamic angles of repose of the particles were measured using ImageJ software. Additionally, the outlines of the particle bed surface, particle displacement, and particle velocity were examined to gain insights into the particle flow phenomena.

The study's findings indicated that as the simulation time increased, the upper angles of repose consistently showed a tendency to increase for all cases. However, the lower angles of repose behaved differently for the alumina particles and the mixture containing 10 % alumina in aluminum alloy particles, exhibiting an opposite trend compared to the lower angles of repose observed in the other three cases.

The s-shaped outline of the powder bed was observed for alumina particles. In the case of mixtures containing aluminum alloy and alumina particles, the bed surfaces closely resembled the pattern of the aluminum alloy, appearing smooth. This similarity can possibly be explained by variations in the particle distribution within the drum due to the different filling levels. The displacement analysis of alumina and aluminum alloy particles in a rotary drum shows that particles in different regions have varying mobility. Alumina particles on the upper side of the drum are more mobile than those on the lower side. Additionally, aluminum alloy particles on the lower side of the drum experience greater displacement compared to alumina particles in the same positions. Particle velocity maps revealed the presence of two distinct layers. In the active layer, particles were observed flowing downward under the influence of gravitational force. Conversely, in the passive layer, particles displayed a tangent velocity that matched the velocity of the drum wall, owing to the no-slip condition at the drum wall.

Acknowledgments

This research was funded by the Science Committee of the Ministry of Education and Science of the Republic of Kazakhstan, grant number AP09260422.

References

1 Sadhu, K.K., Mandal, N. & Sahoo, R.R. (2023). SiC/graphene reinforced aluminum metal matrix composites prepared by powder metallurgy: A review. *Journal of Manufacturing Processes, 91*, 10-43. doi:10.1016/j.jmapro.2023.02.026.

2 Malaki, M., Tehrani A.F. & Niroumand, B. (2020). Fatgiue behavior of metal matrix nanocomposites. *Ceramics International, 46*(15), 2020, 23326-23336. doi:10.1016/j.ceramint.2020.06.246.

3 Aramideh, S., Xiong, Q., Kong, S.-C. & Brown, R.C. (2015). Numerical simulation of biomass fast pyrolysis in an auger reactor. *Fuel,156*, 234-242. doi:10.1016/j.fuel.2015.04.038.

4 Sinnott, M.D. & Cleary, P.W. (2016). The effect of particle shape on mixing in a high shear mixer. *Computational Particle Mechanics, 3*, 477–504. doi:10.1007/s40571-015-0065-4.

5 Höhner, D., Wirtz, S. & Scherer, V. (2015). A study on the influence of particle shape on the mechanical interactions of granular media in a hopper using the Discrete Element Method. *Powder Technology, 278*, 286-305. doi:10.1016/j.powtec.2015.02.046.

6 Hua, X., Curtis, J., Hancock, B., Ketterhagen, W. & Wassgren, C. (2013). The kinematics of non-cohesive, sphero-cylindrical particles in a low-speed, vertical axis mixer. *Chemical Engineering Science, 101*, 144-164.doi:10.1016/j.ces.2013.05.063.

7 Chung, Y., Yeh, C. & Liao, C. (2022). Experimental investigation into the wet non-spherical granular segregation and mixing in rotating drums. *Powder Technology, 409*, 117844. doi:10.1016/j.powtec.2022.117844.

8 He, S.Y., Gan, J.Q., Pinson, D., Yu, A.B. & Zhou, Z.Y. (2019). Radial segregation of binary-sized ellipsoids in a rotating drum.*Powder Technology, 357*, 322-330. DOI: 10.1016/j.powtec.2019.08.075.

9 Chen, H., Xiao, Y.G., Liu, Y.L. & Shi, Y.S. (2017). Effect of Young's modulus on DEM results regarding transverse mixing of particles within a rotating drum. *Powder Technology, 318*, 507-517.doi: 10.1016/j.powtec.2017.05.047.

10 Norouzi, H.R., Zarghami, R. & Mostoufi, N. (2015). Insights into the granular flow in rotating drums. *Chemical Engineering Research and Design, 102*, 12-25.doi: 10.1016/j.cherd.2015.06.010.

11 He, S.Y., Gan, J.Q., Pinson, D., Yu, A.B. & Zhou, Z.Y. (2021). Particle shape-induced axial segregation of binary mixtures of spheres and ellipsoids in a rotating drum. *Chemical Engineering Science, 235*, 116491. DOI: 10.1016/j.ces.2021.116491.

12 Cundall, P.A. & Strack, O.D.L. (1979). A discrete numerical model for granular assemblies. *Géotechnique, 29*(1), 1751-7656. DOI: 10.1680/geot.1979.29.1.47

13 Iwashita, K. & Oda, M. (2000). Micro-deformation mechanism of shear banding process based on modified distinct element method. *Powder Technology, 109*(1–3), 192-205. doi:10.1016/S0032-5910(99)00236-3

14 Ai, J., Chen, J.-F., Rotter, J.M. & Ooi, J.Y. (2011). Assessment of rolling resistance models in discrete element simulations. *Powder Technology, 206*(3), 269-282. doi:10.1016/j.powtec.2010.09.030.

15 Han, Y., Zhao, D., Jia, F., Qui, H., Li, A. & Bai, S. (2020). Experimental and numerical investigation on the shape approximation of rice particle by multi-sphere particle models. *Advanced Powder Technology*, *31*(4), 1574-1586. doi:10.1016/j.apt.2020.01.025.

16 Berkinova, Z., Yermukhambetova, A. & Golman, B. (2021). Simulation of flow properties of differently shaped particles using the discrete element method.*Computer Applications in Engineering Education, 29*(5), 1061-1070. doi:10.1002/cae.22359.

17 Wang, S., Zhou, Z. & Ji, S. (2021). Radial segregation of a gaussian-dispersed mixture of superquadric particles in a horizontal rotating drum. *Powder Technology, 394*, 813-824. doi:10.1016/j.powtec.2021.09.012.

18 Boribayeva, A., Iniyatova, G., Uringaliyeva, A. & Golman, B. (2021). Porous Structure of Cylindrical Particle Compacts. *Micromachines, 12*(12), 1498. doi:10.3390/mi12121498.

19 Iniyatova, G., Yermukhambetova, A., Boribayeva, A. & Golman, B. (2023). Approximate Packing of Binary Mixtures of Cylindrical Particles. *Micromachines, 14*(1), 36. DOI: 10.3390/mi14010036.

20 Buša, J., Džurina, J., Hayryan, E., Hayryan, S., Hu, C.-K., Plavka, J., Pokorný, I., Skřivánek, J. & Wu, M.-C. (2005). ARVO: A Fortran package for computing the solvent accessible surface area and the excluded volume of overlapping spheres via analytic equations. *Computer Physics Communications, 165*(1), 59-96. doi:10.1016/j.cpc.2004.08.002.

21 Marigo, M. & Stitt, E.H. (2015). Discrete element method (DEM) for industrial applications: comments on calibration and validation for the modelling of cylindrical pellets. *KONA Powder and Particle Journal, 32*, 236–252.doi:10.14356/kona.2015016.

22 Jadidi, B., Ebrahimi, M., Ein-Mozaffari, F. & Lohi, A. (2022). Mixing performance analysis of non-cohesive particles in a double paddle blender using DEM and experiments. *Powder Technology, 397*, 117122. doi:10.1016/j.powtec.2022.117122.

23 Mellmann, J. (2001).The transverse motion of solids in rotating cylinders—forms of motion and transition behavior. *Powder Technology. 118*(3), 251-270. doi:10.1016/S0032-5910(00)00402-2.

24 Henein, H., Brimacombe, J.P. & Watkinson, A.P. (1983). Modelling Transverse Motion of Solids in Rotary Kilns. *Metallurgical TransactionB*, *14B*(2), 207-220.

25 Zhu, L., Lu, H., Guo, X. & Liu, H. (2022). Structural relaxation and avalanche dynamics of particle piles under vertical vibration. *Particuology, 68*, 65-74. doi:10.1016/j.partic.2021.11.002.https://doi.org/10.1016/j.partic.2021.11.002

Ж. Беркинова, Б. Гольман

Айналмалы барабандардағы күрделі пішінді бөлшектер қоспаларының ағыс сипаттамасы Дискреттік элементтер әдісі бойынша зерттеу

Металл матрицалық композиттер энергияны үнемдеу саласында қолдануға арналған функционалды материалдар ретінде үлкен әлеуетке ие. Бұл композиттер ұнтақты металлургия әдістерімен, яғни әртүрлі формалары бар ұсақ бөлшектерді қолдана отырып жасалады. Әртүрлі пішіндегі бөлшектер қоспаларының ағындылығын түсіну өнеркәсіптік процестерді оңтайландыру үшін өте маңызды. Мақалада дискретті элементтер әдісін қолдана отырып, алюминий оксиді мен алюминий қорытпасының бөлшектерінен тұратын қоспалар ағысының өтімділігі мен сипаттамалары қарастырылған. Бөлшектердің пішіндері барынша шынайы бөлшек пішіндеріне ұқсастырып алынады және олардың айналмалы барабандағы ағысының әрекеті симуляцияланады. Күрделі пішінді бөлшектердің ағысын сипаттау үшін бөлшек қабатының жоғарғы және төменгі көлбеу динамикалық бұрыштары, бөлшектер қабат бетінің контурлары, бөлшектердің орын ауыстыруы және жылдамдықтарының таралымы талданған. Бөлшектердің пішіндері ұнтақ қоспаларының ағысының әрекетіне әсер ететінін растайтын талдау нәтижелері процестерді оңтайландыру және жобалау үшін пайдалы ақпарат береді.

Кілт сөздер: күрделі пішінді бөлшектер, ұнтақ қоспалары, металл матрицалық композиттер, айналмалы барабан, дискретті элементтер әдісі, аққыштық, динамикалық көлбеу бұрышы, ағыс сипаттамасы.

Ж. Беркинова, Б. Гольман

Характеристики течения смесей частиц сложной формы во вращающихся барабанах Исследование методом дискретных элементов

Металлические матричные композиты обладают большим потенциалом в качестве функциональных материалов для применения в области энергосбережения. Эти композиты производятся методами порошковой металлургии, с использованием мелких частиц с различными формами. Понимание текучести смесей частиц с различными формами является важным для оптимизации промышленных процессов. В статье изучены текучесть и характеристики течения потока смесей, состоящих из частиц оксида алюминия и алюминиевого сплава, с применением метода дискретных элементов. Формы частиц моделируются таким образом, чтобы максимально приблизить их к реальным частицам, и их поведение при движении потока частиц во вращающемся барабане симулируется. Верхний и нижний углы откоса, контуры поверхности слоя частиц, перемещения частиц и распределения скорости частиц проанализированы для понимания характеристик потока частиц сложной формы. Результаты анализа, подтверждающие, что формы частиц влияют на поведение потока смесей порошков, дают полезную информацию для оптимизации и проектирования процессов.

Ключевые слова: частицы сложной формы, смеси порошков, металлические матричные композиты, вращающийся барабан, метод дискретных элементов, текучесть, динамический угол откоса, характеристика течения.